Intratumoral Distribution of Radiolabeled Antibody and Radioimmunotherapy in Experimental Liver Metastases Model of Nude Mouse

Noriko Sato, Tsuneo Saga, Harumi Sakahara, Zhengsheng Yao, Yuji Nakamoto, Meili Zhang, Masahide Kuroki, Yuji Matsuoka, Yasuhiko Iida and Junji Konishi

Department of Nuclear Medicine and Diagnostic Imaging, Kyoto University, Kyoto; and First Department of Molecular Biology, Fukuoka University, Fukuoka, Japan

The biodistribution and intratumoral distribution of radiolabeled anticarcinoembryonic antigen (CEA) monoclonal antibody in experimental liver metastases and the therapeutic effect of ^{131}I-labeled anti-CEA antibody on the metastases were studied. **Methods:** Three weeks after an intrasplenic injection of human colon cancer cells, mice received an intravenous injection of ^{125}I- or ^{111}In-labeled anti-CEA antibody F33–104. The biodistribution and tumor penetration of radiolabeled antibody were examined by using quantitative autoradiography. To evaluate the therapeutic effect, 5.55, 9.25 or 11.1 MBq (150, 250 or 300 μCi) ^{131}I-labeled F33–104 were injected into groups of mice that had micrometastases smaller than 1 mm. Control groups were injected with phosphate-buffered saline or ^{131}I-labeled control antibody. Mice were killed 3 wk later to determine the size of liver metastases. **Results:** ^{125}I-labeled F33–104 showed a high accumulation in the liver metastases (percentage of injected dose per gram of metastases [%ID/g] >24%, metastasis-to-liver ratio >9.8, metastasis-to-blood ratio >2.1); however, its accumulation was heterogeneous or peripheral in the nodules more than 1 mm in diameter. When the antibody dose was increased, antibody penetration was improved, but tumor uptake of radioactivity and specificity ratios decreased. In mice with large metastases, radioactivity in the normal tissue was lower than that in mice with small metastases, resulting in higher metastasis-to-background ratios. ^{111}In-labeled antibody showed even higher tumor uptake than ^{125}I-labeled antibody (>51 %ID/g). Metastases formation was suppressed in a dose-dependent manner by ^{131}I-labeled F33–104 injection (5 of 8 mice had no macroscopic tumor after an injection of 5.55 MBq (150 μCi), and all mice had no visible metastasis after an injection of 9.25 or 11.1 MBq [250 or 300 μCi]), whereas tumor progression was seen in the control groups. **Conclusion:** Liver metastases had easy accessibility to the antibody. Micrometastases of less than 0.5 mm in diameter showed homogeneous intratumoral distribution of injected antibody and were successfully treated with ^{131}I-labeled antibody. Very high uptake and satisfactory metastasis-to-liver ratios with ^{111}In-labeled antibody suggest that the use of a radiometal with high β-energy, such as ^{90}Y or ^{188}Re, is preferable for the successful radioimmunotherapy of metastases larger than 1 mm.

Key Words: radioimmunotherapy; antibody; liver metastasis; colon cancer; biodistribution

J Nucl Med 1999; 40:685–692

For the treatment of metastatic lesions of malignant tumors, various therapies such as surgery, chemotherapy, radiotherapy and hormone therapy have been tried, but they remain of limited value (*1,2*). Radioimmunotherapy (RIT) is theoretically an appropriate method for treating metastases, because cancer-specific antibodies can selectively deliver cytotoxic radioisotopes to the widespread metastatic foci, even if they are invisible, exerting a direct irradiation effect on tumor cells with minimal damage to normal tissues.

Although the RIT of malignant lymphomas has been shown to be a promising mode of therapy, RIT of more common solid cancers has not been effective enough. In contrast to hematological malignancies, which are highly radiosensitive and in which the antigen is readily accessible to a blood-borne antibody, solid tumors are rather radioresistant and their macromolecule accessibility is poor (*1,2*), especially when the tumors have grown large. Previous experimental RIT trials were performed against large tumors, and have shown only transient remission, even with the administration of the maximal tolerated dose (*3*). A reduction of severe bone marrow toxicity was produced by repeated administration of radiolabeled antibody (*4*), but was still insufficient. Small tumors, in contrast, are expected to show a higher and more homogeneous radioactivity uptake (*5–7*), and recent RIT trials for such small tumors have presented encouraging results (*8,9*). Because high tumor uptake with high tumor-to-normal tissue ratios and a homogeneous accumulation of radiolabels in the tumors are essential for the RIT to be successful, small metastatic lesions would seem to be the optimal candidate for RIT.

Received Feb. 19, 1998; revision accepted Aug. 4, 1998.

For correspondence or reprints contact: Noriko Sato, MD, Department of Nuclear Medicine and Diagnostic Imaging, Faculty of Medicine, Kyoto University, 54 Kawahara, Shogoin, Sakyo, Kyoto 606–8507, Japan.

The liver metastasis model of mice, established by injecting tumor cells into spleen or cecum (*10–12*), is closer to the clinical situation than the usual subcutaneous tumor model. Vogel et al. (*13*) recently reported favorable biodistribution properties of small liver metastasis (high tumor uptake, easy antibody accessibility), but the biodistribution of radiolabeled antibody in the metastasis was heterogeneous (*13*). In this study, the biodistribution and spacial distribution of a radiolabeled anticancer monoclonal antibody (MoAb) in the experimental liver metastasis were evaluated, focusing on the effects of the antibody dose and tumor size on the biodistribution and intratumoral microdistribution of the radiolabels. In addition, the short-term therapeutic effect of an intravenously injected ^{131}I-labeled MoAb was examined in a micrometastasis model.

MATERIALS AND METHODS

Cell Lines

The carcinoembryonic antigen (CEA)-expressing human colorectal carcinoma cell lines LS174T and LS180 were obtained from the American Type Culture Collection (Rockville, MD). Cells were grown in RPMI 1640 medium (Nissui Pharmaceutical Co., Tokyo, Japan) supplemented with 10% fetal calf serum (GIBCO Laboratories, Grand Island, NY) and 0.03% L-glutamine, in a 5% CO_2 environment. Subconfluent cells were detached with calcium- and magnesium-free phosphate-buffered saline (PBS) containing 0.02% ethylenediaminetetraacetic acid (EDTA) with or without 0.05% trypsin, and then used for the in vitro and in vivo studies.

Liver Metastases Model

Female BALB/c nu/nu mice were anesthetized with ether inhalation, and the spleen was exteriorized through a short left subcostal incision. A single-cell suspension of 3×10^6 LS174T cells in 50 μL serum-free RPMI 1640 medium was slowly injected into the spleen though a 27-gauge needle, followed 2 min later by splenectomy. The left subcostal incision was closed with metal clips (*14*).

Monoclonal Antibodies

The murine IgG_1 MoAb–designated F33–104 recognizes the CEA-specific proteinaceous part of the CEA molecule (*15, 16*). The MoAb 56C, which is also a murine IgG_1 recognizing human chorionic gonadotropin, was used as an isotype-matched control antibody. The antibodies were purified from the ascitic fluid of hybridoma-bearing mice, with protein A affinity chromatography (Bio-Rad, Richmond, CA).

Radiolabeling

Antibodies were radioiodinated with the chloramine-T method (*17*). Fifty micrograms of purified antibody in 200 μL 0.3 mol/L phosphate buffer, pH 7.5, and 11.1 MBq (300 μCi) ^{125}I (Du Pont, Wilmington, DE) were mixed with 2.5 μg chloramine-T (Nacalai Tesque, Kyoto, Japan), dissolved in 0.3 mol/L phosphate buffer. After 5 min, radiolabeled antibodies were separated from the free iodine though PD-10 gel chromatography (Pharmacia LKB Biotechnology, Uppsala, Sweden). The specific activities of ^{125}I-labeled antibodies ranged from 79.6–167.2 MBq/mg (2.2–4.5 mCi/mg). Antibodies were also ^{131}I-labeled by the chloramine-T method.

F33–104 antibody was also labeled with ^{111}In by using 1-(4-isothiocyanatobenzyl) ethylenediamine-N,N,N′,N′-tetraacetic acid (SCN-Bz-EDTA; Dojindo Co., Kumamoto, Japan) as a bifunctional chelating agent, according to the method of Brechbiel et al. (*18*) and Esteban et al. (*19*) with some modifications (*20*). Briefly, antibody solutions (11 mg/mL) in 0.05 mol/L borate-buffered saline, pH 8.5, were mixed with SCN-Bz-EDTA dissolved in dimethylformamide with the mixing molar ratio of 1:5 and incubated overnight at 30°C. The unconjugated SCN-Bz-EDTA was removed by applying the mixture to the PD-10 gel chromatography with 20 mmol/L 2 N-morpholino ethanesulfolic acid-buffered saline (MES), pH 6.0, as an eluant. The conjugation ratio of the antibody was calculated to be 1.58. Conjugated antibodies (200 μg/100 μL in MES) were mixed with 13.6 MBq (367.6 μCi) ^{111}In-labeled acetate, which was prepared by adding 40 μL 1.75 mol/L HCl and 160 μL 1 mol/L sodium acetate to 200 μL ^{111}In-labeled chloride (Nihon Mediphysics, Nishinomiya, Japan). The labeling efficiency was more than 99%.

The immunoreactivities of ^{125}I-, ^{131}I- and ^{111}In-labeled antibodies were measured using LS180 cells according to the method of Lindmo et al. (*21*) and were always more than 68% for each preparation. Radiolabeled 56C showed no specific binding to LS180 cells.

Biodistribution Study

Three weeks after the intrasplenic injection of LS174T cells, the mice received an intravenous injection of ^{125}I-labeled F33–104 antibody (148 kBq [4 μCi]/10 or 100 μg) or ^{111}In-labeled MoAb (148 kBq [4 μCi]/10 μg). Ten micrograms of antibody corresponds to the dose necessary to saturate the binding site of a 0.1-g tumor, and 100-μg of antibody to a 1-g tumor. The mice were killed 24, 48 or 96 h postinjection by ether inhalation. Livers with metastases were removed and quickly frozen in OCT compound (Tissue Tec; Miles Inc., Elkhart, IN) from which 15-μm thick sections were made and processed for quantitative autoradiography (QAR) study. Blood and various organs were removed and weighed, and their radioactivity counts were determined. The percentages of injected dose per gram of tissue (%ID/g) were determined by QAR for the liver and liver tumors and by direct tissue counting for the other organs, and were normalized to a 20-g mouse. Metastases-to-normal tissue ratios of radioactivity were also calculated. All animal experiments were performed in accordance with the Japanese regulations regarding animal care and handling.

Quantitative Autoradiography

The uptake and penetration of radiolabeled antibody into the metastatic nodules were evaluated with QAR. Dried 15-μm frozen sections of the liver with metastases were placed in a light-tight cassette along with ^{125}I- or ^{111}In-calibrated standards in direct contact with Kodak X-OMAT XAR film (Eastman Kodak, Rochester, NY). ^{125}I- and ^{111}In-calibrated standards were prepared as described previously (*22*). After 4–6 d of exposure at room temperature, the films were processed through an automatic developer.

The autoradiographic images were digitized with a videodensitometry system (EXCEL TVIP-4100; Nippon Avionics, Tokyo, Japan). Standard curves were obtained from the optical densities measured on the standards. Then, regions of interest were drawn over each metastatic nodule and over a normal liver by referring to the hematoxylin and eosin staining of the same section. The optical densities of these regions were converted to radioactivity per gram by using the standard curve. The background of the film itself was subtracted.

The autoradiographic pattern of microdistribution of the radiolabel was analyzed visually and also analyzed by semiquantitative

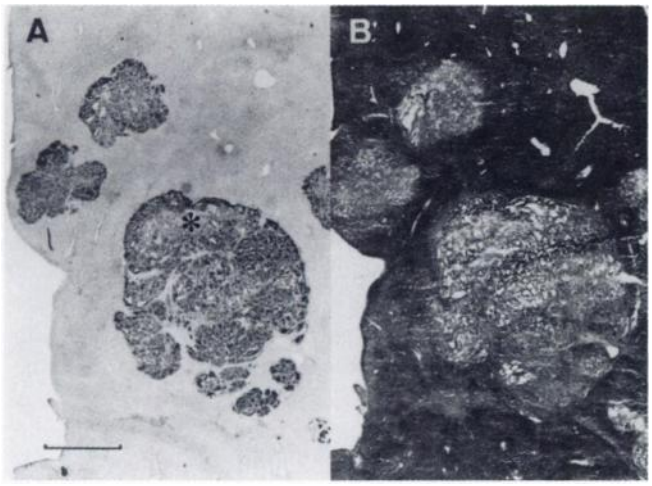

FIGURE 1. Immunohistochemical (A) and hematoxylin and eosin staining (B) of liver with metastases 3 wk after intrasplenic injection of cancer cells. Immunohistochemical staining shows diffuse expression of CEA in each metastatic nodule of varying size, except for necrotic areas seen in upper part of largest nodule (*). Original magnification 2.5×. Bar indicates 1 mm.

morphometrical analysis. The patterns of radioactivity distribution observed were divided into three categories: marginal, radioactivity found only at the nodular margin; diffuse heterogeneous, radioactivity found throughout the nodule but distributed very heterogeneously; and diffuse homogeneous, radioactivity found throughout the nodule and distributed more homogeneously. Each nodule was classified according to its diameter and to the radioactivity distribution pattern.

Radioimmunotherapy

Two series of the RIT experiment were performed for small micrometastases. In the first experiment, 7 d after the intrasplenic grafting of LS174T cells, mice (n = 8) received an intravenous injection of 5.55 or 11.1 MBq (150 or 300 μCi, 26 μg) ^{131}I-labeled F33–104. The control group of mice received PBS instead of ^{131}I-labeled antibody. In the second experiment, 9.25 MBq (250 μCi, 26 μg) ^{131}I-labeled F33–104 or ^{131}I-labeled control 56C antibody or PBS was injected intravenously (n = 6). Mice in both series were killed 3 wk after the intravenous injection (i.e., 4 wk after the intrasplenic tumor grafting) to examine the formation of liver metastases. In both experiments, another group of mice received an intravenous injection of ^{125}I-labeled F33–104 and were killed 1 or 2 d later to check the formation of metastasis and to confirm the localization of radiolabeled F33–104 in the metastatic nodules. The results of the radioimmunotherapy were analyzed by Mann-Whitney test with Bonferroni correction. Analyses were performed with a grading of the metastasis: small tumor, intermediate tumor, large tumor (the same grading as in the biodistribution study) and nonvisible tumor. A corrected probability value of less than 0.05 was considered significant.

RESULTS

Experimental Liver Metastases

After injection of 3 × 10^6 cancer cells, all the mice developed multiple liver metastases of varying sizes. The expression of CEA in each metastasis was diffuse, except for the necrotic parts in larger nodules, as shown by immunohistochemical staining with anti-CEA antibody as a primary antibody (Fig. 1).

Biodistribution of ^{125}I- and ^{111}In-labeled F33–104

The biodistribution data of ^{125}I-labeled F33–104 in nude mice with liver metastases are summarized in Table 1. Because the size of the metastatic nodules and the total amount of metastases varied among the mice studied, the

TABLE 1
Biodistribution of ^{125}I-labeled Murine IgG_1 Monoclonal Antibody F33-104 in Liver Metastases Model of Nude Mouse

	Small tumor*				Large tumor†			
	10 μg		100 μg		10 μg		100 μg	
	24 h (n = 6)	96 h (n = 5)	24 h (n = 5)	96 h (n = 6)	24 h (n = 3)	96 h (n = 3)	24 h (n = 5)	96 h (n = 6)
%ID/g‡								
Blood	11.72 ± 1.74	7.42 ± 2.55	13.22 ± 1.45	6.28 ± 3.24	3.27 ± 0.78	0.35 ± 0.19	5.73 ± 3.17	2.14 ± 2.13
Kidney	3.25 ± 0.64	2.21 ± 0.87	3.74 ± 0.28	1.77 ± 0.94	1.46 ± 0.19	0.19 ± 0.06	2.06 ± 1.05	0.67 ± 0.53
Lung	4.85 ± 0.66	3.19 ± 1.25	5.21 ± 0.90	2.65 ± 1.53	1.83 ± 0.30	0.23 ± 0.12	2.68 ± 1.54	1.02 ± 0.82
Muscle	1.23 ± 0.33	0.71 ± 0.38	1.15 ± 0.17	0.63 ± 0.35	0.64 ± 0.15	0.07 ± 0.04	0.64 ± 0.23	0.30 ± 0.19
Bone	1.57 ± 0.52	0.90 ± 0.53	1.78 ± 0.37	0.79 ± 0.62	0.83 ± 0.18	0.09 ± 0.03	0.89 ± 0.49	0.33 ± 0.25
Liver	2.62 ± 0.62	1.65 ± 0.39	2.68 ± 0.97	1.69 ± 0.38	2.05 ± 0.34	1.24 ± 0.58	2.79 ± 1.63	1.22 ± 0.64
Tumor	24.43 ± 5.59	27.31 ± 10.24	15.32 ± 3.19	12.80 ± 4.60	30.75 ± 10.73	12.30 ± 3.64	23.21 ± 4.98	13.38 ± 6.47
Tumor-to-nontumor ratio‡								
Blood	2.12 ± 0.56	4.03 ± 2.27	1.15 ± 0.13	2.23 ± 0.51	10.31 ± 5.98	38.07 ± 8.36	8.54 ± 11.86	16.69 ± 18.18
Kidney	7.77 ± 2.19	13.81 ± 8.26	4.08 ± 0.60	7.92 ± 1.72	21.91 ± 10.72	66.02 ± 3.60	17.63 ± 18.77	32.13 ± 24.08
Lung	5.10 ± 1.16	9.58 ± 5.97	2.93 ± 0.18	5.42 ± 1.31	17.77 ± 9.49	58.40 ± 13.40	14.47 ± 16.21	21.47 ± 16.56
Muscle	20.69 ± 5.89	48.31 ± 38.38	13.32 ± 1.60	22.35 ± 5.04	51.81 ± 29.59	180.17 ± 41.77	44.78 ± 32.32	56.15 ± 26.53
Bone	16.98 ± 6.71	40.19 ± 33.92	8.84 ± 2.09	22.25 ± 9.67	39.20 ± 20.83	134.78 ± 46.18	40.38 ± 41.75	69.97 ± 61.15
Liver	9.83 ± 3.11	17.55 ± 8.66	5.92 ± 0.81	7.44 ± 1.43	15.90 ± 8.51	12.98 ± 10.04	9.86 ± 3.59	11.40 ± 2.48

*Less than 2 mm in diameter.
†More than 40% of liver surface with or without bloody ascites.
‡Results given as mean ± SD.

mice were divided into three groups according to the grade of metastasis: small tumor, multiple small metastases less than 2 mm in diameter; large tumor, metastases have become larger and confluent to occupy more than 40% of the surface of the liver; and intermediate tumor, between a small tumor and large tumor. To make the comparison easier, data from the small tumor and large tumor groups were compared. A comparison was also made between low-dose (10 μg) and high-dose (100 μg) injection groups.

After the injection of 10 μg ^{125}I-labeled F33–104 into mice with small metastases, tumor uptake was as high as 24.4% at 24 h, and this high uptake was maintained at 96 h after injection. The blood and normal tissue uptakes decreased with time, resulting in tumor-to-blood ratio increases from 2.1 at 24 h to 4.0 at 96 h and tumor-to-liver ratio increases from 9.8 at 24 h to 17.6 at 96 h after injection. When a high dose (100 μg) of antibody was injected, the tumor uptake of radioactivity significantly decreased, resulting in lower tumor-to-blood and tumor-to-normal tissue ratios compared with the low-dose groups.

In the mice with large metastases, blood clearance of the antibody was much faster than that observed in the mice with small metastases. A high 30.8% tumor uptake at 24 h suggested that the antibody was easily accessible to the metastatic nodules in the liver, and a large amount of antibody was rapidly taken up by the metastases. The faster blood clearance may also be due to the higher complexing of circulating antibody with CEA molecules shed from large tumors and rapid elimination of complexes through the reticuloendothelial system.

^{111}In-labeled F33–104 showed much higher tumor uptake than ^{125}I-labeled antibody at every time point and also a gradual increase up to 92.1% at 96 h postinjection, with a tumor-to-blood ratio of 9.9 (Table 2). The tumor-to-liver ratio also remained high (5.2 at 24 h and 8.9 at 96 h).

TABLE 2
Biodistribution of ^{111}I-labeled F33-104 in Nude Mice

	24 h (n = 3)	48 h (n = 6)	96 h (n = 6)
%ID/g*			
Blood	15.88 ± 1.37	13.41 ± 2.03	9.47 ± 1.48
Kidney	5.69 ± 0.07	5.03 ± 0.53	3.77 ± 0.64
Lung	5.89 ± 0.62	6.29 ± 1.26	4.45 ± 0.56
Muscle	1.35 ± 0.17	1.16 ± 0.08	0.93 ± 0.16
Bone	1.84 ± 0.45	1.79 ± 0.15	1.68 ± 0.32
Liver	10.00 ± 0.79	10.24 ± 1.61	10.67 ± 2.88
Tumor	51.76 ± 4.39	55.87 ± 7.75	92.06 ± 13.96
Tumor-to-nontumor ratio*			
Blood	3.29 ± 0.54	4.22 ± 0.70	9.89 ± 1.91
Kidney	9.10 ± 0.87	11.13 ± 1.30	24.86 ± 4.87
Lung	8.90 ± 1.58	9.12 ± 1.72	21.00 ± 3.98
Muscle	39.01 ± 7.76	48.27 ± 8.09	102.00 ± 24.96
Bone	29.43 ± 8.34	31.44 ± 5.47	56.74 ± 14.15
Liver	5.18 ± 0.30	5.53 ± 0.86	8.86 ± 1.22

*Results are given as mean ± SD.

Intratumoral Distribution of Radiolabeled F33–104

The spatial distribution of ^{125}I-labeled F33–104 was determined by autoradiography. Representative images are shown in Figure 2.

When low-dose (10 μg) ^{125}I-labeled F33–104 was administered, the radioactivity was localized in the periphery of each metastatic nodule at 24 h (Fig. 2A). Even at 96 h, penetration of the antibody was not sufficient in the relatively larger metastatic nodules (Fig. 2B). When the dose of the antibody was increased (100 μg), penetration of the antibody was improved, especially at 96 h (Fig. 2C, D). However, the grain density was lower in accordance with the decreased radioactivity uptake in the metastatic lesions (Table 1). Examples of the three categories of intratumoral radioactivity distribution pattern, diffuse homogeneous, diffuse heterogeneous and marginal, are indicated (Fig. 2, a–c).

These qualitative findings of the ^{125}I-labeled F33–104 microdistribution are substantiated by semiquantitative morphometric analysis, as shown in Table 3. In the metastatic nodules larger than 1 mm in diameter, the distribution of low-dose antibody was marginal in most nodules at 24 h; even at 96 h, only half of the nodules showed the diffuse

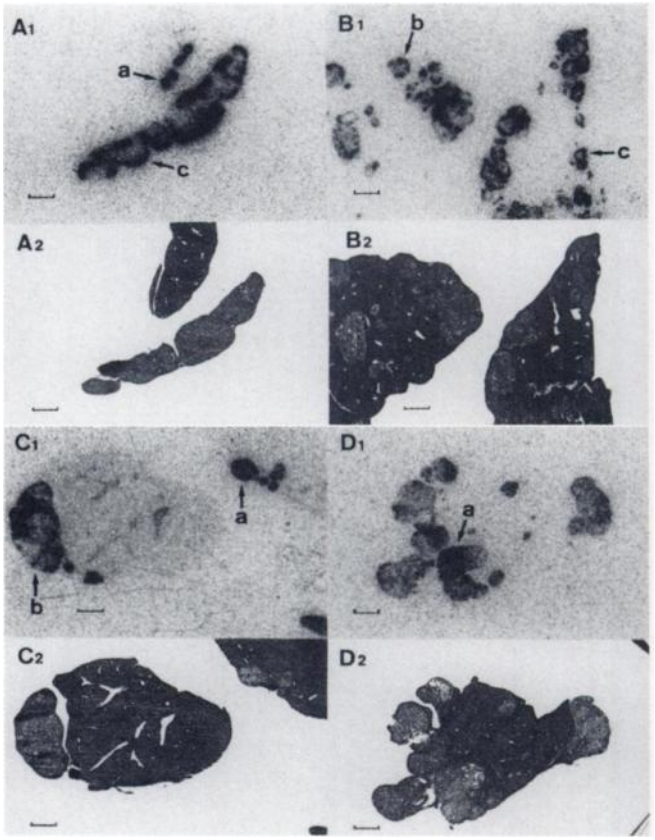

FIGURE 2. Autoradiography (A_1–D_1) and hematoxylin and eosin staining (A_2–D_2) of liver with metastases obtained 24 (A, C) and 96 h (B, D) after injection of 10 μg (A, B) and 100 μg (C, D) ^{131}I-labeled F33–104. Examples of three categories of intratumoral radioactivity distribution pattern are shown: diffuse homogeneous (a), diffuse heterogeneous (b) and marginal (c). Original magnification 2.5×. Bars indicate 1 mm.

TABLE 3
Semiquantitative Analysis of the Intratumoral Biodistribution of ^{125}I-labeled F33-104

Tumor size (mm)	Low dose (10 μg)		High dose (100 μg)	
	24 h	96 h	24 h	96 h
≤0.5				
A*	73 (36/49)§	79 (44/56)	93 (64/69)	92 (119/130)
B†	12 (6/49)	16 (9/56)	3 (2/69)	8 (10/130)
C‡	14 (7/49)	5 (3/56)	4 (3/69)	1 (1/130)
0.5–1.0				
A	12 (6/52)	28 (12/43)	42 (31/73)	68 (86/127)
B	29 (15/52)	37 (16/43)	42 (31/73)	28 (35/127)
C	60 (31/52)	35 (15/43)	15 (11/73)	5 (6/127)
1.0–2.0				
A	0 (0/34)	13 (3/23)	33 (19/57)	41 (39/94)
B	12 (4/34)	30 (7/23)	30 (17/57)	45 (42/94)
C	88 (30/34)	57 (13/23)	37 (21/57)	14 (13/94)
2.0<				
A	0 (0/12)	20 (4/20)	6 (2/36)	20 (6/30)
B	8 (9/12)	30 (6/20)	47 (17/36)	73 (22/30)
C	92 (11/12)	50 (10/20)	47 (17/36)	7 (2/30)

*Diffuse homogeneous.
†Diffuse heterogeneous.
‡Marginal.
§% (nodules/nodules in each size).

pattern and less than 20% presented the homogeneous pattern of distribution. Smaller nodules (less than 1 mm in diameter) showed better penetration but very little homogeneity. When the high dose of antibody was injected, the penetration of radiolabels was significantly improved, and most nodules presented the diffuse heterogeneous or diffuse homogeneous pattern, although the fraction of the nodules showing the diffuse homogeneous pattern was not high. Of the nodules less than 0.5 mm in diameter, most showed the homogeneous pattern even with the low dose of antibody; however, this may be an overestimation because nodules cut off center were included in this group and were regarded as showing homogeneous distribution.

The intratumoral distribution of ^{111}In-labeled F33–104 was also studied, and was found to be almost identical to that of ^{125}I-labeled F33–104 (data not shown).

Radioimmunotherapy

In the two series of RIT experiments, the intravenous injection of ^{131}I-labeled MoAb was well tolerated by all the mice.

Figure 3 shows the autoradiography of the liver with metastases obtained 2 d after intravenous injection of ^{125}I-labeled F33–104, which was administered at the same time as the ^{131}I-labeled F33–104 injection of RIT groups. As shown in Figure 3A, at the time when the ^{131}I-labeled antibody was administered for RIT (7 d after intrasplenic grafting of cancer cells), multiple metastases of several hundred microns in diameter were formed in the liver. The autoradiography shows that the injected ^{125}I-labeled F33–104 localized well and was homogeneously distributed within each nodule (Fig. 3B). Table 4 summarizes the results of the RIT experiment. In both experiments, when PBS was injected, all the mice had visible metastases at the time of death, and 11 of these 14 control mice showed massive metastases with bloody ascites. Four mice died before they could be killed. ^{131}I-labeled F33–104 showed a therapeutic effect in a dose-dependent manner. After the injection of 9.25 and 11.1 MBq (250 and 300 μCi) ^{131}I-labeled antibody, no mouse had visible metastasis in the liver. After the administration of 5.5 MBq (150 μCi) antibody, however, 3 of 8 mice had small metastatic nodules. Mice that had received ^{131}I-labeled 56C control antibody presented various grades of metastases, although the grades were less than those of the control (PBS) group. Statistical analysis showed significant therapeutic effect of anti-CEA antibody compared with control (PBS) or control antibody.

DISCUSSION

RIT is theoretically an appropriate method of cancer treatment, because radiolabeled antibodies that bind to the antigen on the cancer cells can directly irradiate tumor cells with minimal irradiation to the normal tissue. For the success of RIT, not only a high tumor uptake and high tumor-to-normal tissue ratios but also a homogeneous accumulation of radiolabels in the tumor are important. It is known, however, that the tumor penetration of radiolabeled antibodies is poor, especially when tumors are large, resulting in an insufficient irradiation of tumor cells far from blood vessels. Various factors are known to affect negatively the penetration of the radiolabeled antibody: poor and heterogeneous vascularization, increased interstitial pres-

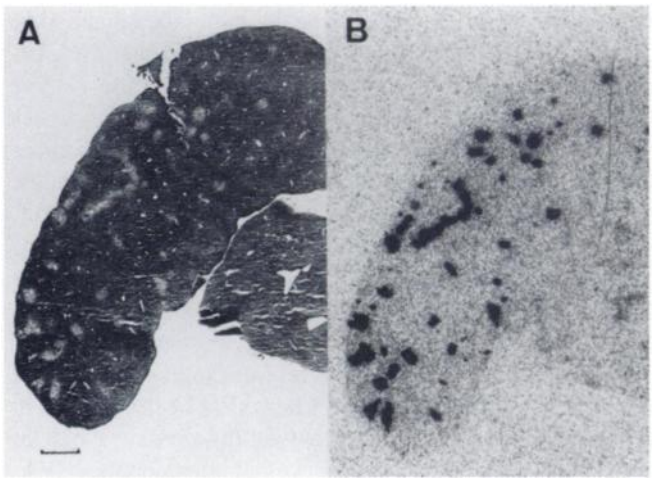

FIGURE 3. Immunohistochemical staining (A) and autoradiogram (B) of liver with metastases obtained 2 d after intravenous injection of ^{125}I-labeled F33–104, which was administered at the same time as ^{131}I-labeled antibody injection of RIT. Multiple metastases of several hundred microns in diameter are seen with good and homogeneous accumulation of ^{125}I-labeled antibody. Original magnification 2.5×. Bar indicates 1 mm.

TABLE 4
Therapeutic Effect of ^{131}I-Labeled F33-104 on Liver Metastases in Nude Mice

First RIT Experiment (n = 8)			
Grade of metastases	Control (PBS)	5.55 MBq ^{131}I-labeled F33-104¶	11.1 MBq ^{131}I-labeled F33-104¶
Nonvisible	0	5	8
Small*	1	3	0
Intermediate†	2	0	0
Large‡	5 (1§)	0	0
Second RIT Experiment (n = 6)			
Grade of metastases	Control (PBS)	9.25 MBq ^{131}I-labeled 56C	9.25 MBq ^{131}I-labeled F33-104**
Nonvisible	0	0	6
Small*	0	1	0
Intermediate†	0	3	0
Large‡	6 (3§)	2	0

*Less than 2 mm in diameter.
†Between small and large tumor.
‡More than 40% of liver surface with or without bloody ascites.
§Died of massive liver metastases with bloody ascites before the day when killed.
¶$P < 0.01$ compared with control.
**$P < 0.01$ compared with control and ^{131}I-labeled 56C.
RIT = radioimmunotherapy; PBS = phosphate-buffered saline.
Groups of mice were administered radiolabeled antibody or PBS 7 days after intrasplenic tumor grafting, and were killed 3 wk later for the determination of the grade of the metastases.

sure in the central portion of the tumor and heterogeneity in antigen expression, among others (*23–25*). Furthermore, the specific binding of the antibody with the target antigen itself may retard further penetration of the radiolabeled antibody (*26–28*). Previous studies have demonstrated that the antibody uptake of small tumors can be higher than that of larger tumors (*6,7,24,29*), and small metastases showed a higher radiolabel uptake compared with the large primary tumors (*24*). Therefore, metastatic nodules are thought to be the best candidates for RIT (*1*).

Experimental liver metastasis models of mice using human colon cancer have been described in SCID or syngenic BALB/c nude mice by injecting tumor cells into the spleen or cecum (*10–12*). A liver metastasis model of colon cancer is a more clinically relevant setting than a usual subcutaneous xenograft model. The LS174T cell line used in this study was derived from a well-differentiated human colon adenocarcinoma and produces a high amount of CEA. It is known that liver metastases can be made with high frequency by LS174T cells compared with other cell lines (*12*). With the injection of 3×10^6 LS174T cells and no pregrafting treatment, all the treated mice showed multiple liver metastases of varying size diffusely expressing CEA antigen, except for the necrotic areas in relatively large tumors. Metastases formation as high as 100% and diffuse antigen expression make this model suitable for the study of RIT with anti-CEA antibody. The spleen was resected after the cell injection to simulate the clinical setting of small liver metastases occurring after resection of the primary lesion.

The anti-CEA antibody presented a high uptake in the tumors with a high metastasis-to-normal tissue ratio. The volume of metastasis significantly affected the biodistribution of radiolabeled F33–104. With an increase in the volume of the metastases, clearance of antibody from blood and normal tissue was markedly facilitated and the tumor uptake was less affected, resulting in higher metastasis-to-background ratios. As pointed out by Vogel et al. (*13*), this may reflect the good accessibility of the liver metastasis to blood-borne antibodies. This is expected because the liver itself is a well-perfused organ and because small metastatic nodules are well vascularized compared with a large subcutaneous xenograft.

^{111}In-labeled F33–104 showed a much higher tumor uptake and a longer retention of radioactivity in metastatic nodules than did ^{125}I-labeled F33–104. This marked difference in tumor uptake seems to be due to the difference in the stability of the radiolabels. ^{111}In-chelation with SCN-Bz-EDTA is quite stable, whereas a radioiodinated antibody prepared by the chloramine-T method is susceptible to dehalogenation.

Despite the high accumulation of F33–104 in tumors, the autoradiography showed heterogeneous or peripheral localization of the low-dose antibody, even in small metastatic lesions of several millimeters in diameter, probably because of the binding-site barrier effect (*26–28*). Increasing the antibody dose overcame this poor penetration somewhat, but resulted in a decreased radiolabel uptake in the metastases and decreased specificity ratios. Decreased specificity ratios cause unnecessary normal tissue radiation, including bone marrow radiation, and make high-dose antibody administration impossible.

Because ^{131}I is a therapeutic radioisotope that can cover only around 1 mm, we selected small 1-wk-old liver micrometastases of submillimeter diameter as the target of RIT using ^{131}I-labeled F33–104. The result of the semiquantitative morphometric analysis of intratumoral distribution of ^{125}I-labeled antibody demonstrated that most of the nodules less than 0.5 mm in diameter showed the homogeneous radiolabel accumulation, and this also suggests the suitability of these micrometastases for RIT. ^{131}I-labeled F33–104 had a dose-dependent inhibitory effect on the liver metastasis. Although only a short-term effect was examined, a high dose (more than 9.25 MBq [250 μCi]) of ^{131}I-labeled F33–104 could effectively control the 1-wk-old liver metastasis. Tumor-size–dependent reduction of effect of a functional RIT of experimental liver metastasis was reported by Vogel et al. (*30*). When RIT was started for a 1-wk-old tumor, suspected to be submillimeter in diameter, the same as that used in this study, the long-term disease-free survival of 6 mo was observed for 8 of 13 mice; however, long-term

survivors significantly reduced to 2 of 14 for a larger 2-wk-old tumor, and no difference in survival was shown with a 3-wk-old tumor compared with untreated mice.

The minor effect on the size of the metastases by the ^{131}I-labeled control antibody might be the nonspecific effect of ^{131}I. Because the radioactivity administered was very high when converted to the radioactivity doses for patients, further improvement is necessary to reduce the administration radioactivity for clinical application.

Several approaches to overcome these problems have been considered and tried (*31*). Antibody fragments penetrated deeper into the tumors than did the intact antibody (*32*). Because of their very short biologic half-life, these antibodies have shown high tumor-to-normal tissue ratios, but on the other hand, the amount of radioactivity accumulated in the tumors was generally very low and required a very high radioactivity administration for therapeutic use (*7,32–35*). The combination of RIT with other therapeutic modalities such as external radiotherapy and chemotherapy has also been tried (*30,36*), but may increase the risk of developing bone marrow toxicity in RIT (*2*). Cytokines to increase tumor blood flow and vascular permeability, to increase antigen expression, to suppress angiogenesis or to protect the bone marrow from irradiation, may be beneficial (*37–40*).

When poor penetration is inevitable, metal nuclides with higher β-energy (i.e., longer effective length) such as ^{90}Y and ^{188}Re are the radioisotopes of choice. The instability and short physical half-life of a ^{188}Re-labeled antibody is another problem (*41*). ^{90}Y has a suitable physical half-life, and a ^{90}Y-labeled antibody prepared with macrocyclic amine was reported fairly stable in vivo (*42*). In this study, ^{111}In-labeled F33–104 showed a much higher tumor uptake than the ^{125}I-labeled antibody (>51 %ID/g). By using SCN-Bz-EDTA as a chelate, the hepatic uptake of ^{111}In was low and the metastasis-to-liver ratio was high (5.18 at 24 h and 8.86 at 96 h). These results indicate that ^{90}Y-labeled F33–104 chelated with macrocyclic amine is promising for the RIT of metastases of several millimeters in diameter.

CONCLUSION

This investigation showed that liver metastasis possessed high accessibility to the antibody and can be a good target of RIT. However, poor penetration of the radiolabeled antibody in metastases of several millimeters in diameter limit the effective use of a ^{131}I-labeled antibody. When ^{131}I is used as a therapeutic radioisotope, even smaller micrometastases with submillimeter diameter are the target of choice, and, in such a situation, the ^{131}I-labeled antibody could effectively control the metastasis. The administered dose, however, was very high and further potentiation of the therapeutic effect is necessary. The very high uptake and satisfactory metastasis-to-liver ratios achieved with the ^{111}In-labeled antibody suggests that the use of a radiometal with high β-energy such as ^{90}Y or ^{188}Re is preferable for the successful RIT of larger metastases.

ACKNOWLEDGMENT

We appreciate Nihon Mediphysics Co. LTD. (Takarazuka, Japan) for generously supplying the $^{111}InCl_3$ used in the investigation.

REFERENCES

1. Behr TM, Goldenberg DM, Becker WS. Radioimmunotherapy of solid tumors: a review "of mice and men." *Hybridoma.* 1997;16:101–107.
2. Behr TM, Sharkey RM, Juweid ME, et al. Phase I/II clinical radioimmunotherapy with an iodine-131-labeled anti-carcinoembryonic antigen murine monoclonal antibody IgG. *J Nucl Med.* 1997;38:858–870.
3. Buchegger F, Rojas A, Delaloye AB, et al. Combined radioimmunotherapy and radiotherapy of human colon carcinoma grafted in nude mice. *Cancer Res.* 1995;55:83–89.
4. Schlom J, Molinolo A, Simpson JF, et al. Advantage of dose fractionation in monoclonal antibody-targeted radioimmunotherapy. *J Natl Cancer Inst.* 1990;82: 763–771.
5. Chatal JF, Douillard JY, Saccavini JC, et al. Clinical prospective study with radioiodinated monoclonal antibodies directed against colorectal cancer. In: Baldwin RW, Byers VS, eds. *Monoclonal Antibodies for Cancer Detection and Therapy.* London: Academic Press; 1985:159–180.
6. Buchegger F, Mach JP, Prèlegrin A, et al. Radiolabeled chimeric anti-CEA monoclonal antibody compared with the original mouse monoclonal antibody for surgically treated colorectal carcinoma. *J Nucl Med.* 1995;36:420–429.
7. Buchegger F, Prèlegrin A, Delaloye AB, Bischof-Delaloye A, Mach JP. Iodine-131-labeled F(ab')^2 fragments are more efficient and less toxic than intact anti-CEA antibodies in radioimmunotherapy of large human colon carcinoma grafted in nude mice. *J Nucl Med.* 1990;31:1035–1044.
8. Cheung N-KV, Landmeier B, Neely J, et al. Complete tumor ablation with iodine 131-radiolabeled disialoganglioside GD_2-specific monoclonal antibody against human neuroblastoma xenografted in nude mice. *J Natl Cancer Inst.* 1986;77:739–745.
9. Senekowitsch R, Reidel G, Möllenstädt S, Kriegel H, Pabst HW. Curative radioimmunotherapy of human mammary carcinoma xenografts with iodine-131-labeled monoclonal antibodies. *J Nucl Med.* 1989;30:531–537.
10. Giaavazzi R, Jessup JM, Campbell DE, Walker SM, Fidler IJ. Experimental nude mouse model of human colorectal cancer liver metastases. *J Natl Cancer Inst.* 1986;77:1303–1308.
11. Bresalier RS, Raper SE, Hujanen ES, Kim YS. A new animal model for human colon cancer metastasis. *Int J Cancer.* 1987;39:625–630.
12. Tibbettes LM, Doremus CM, Tzanakakis GN, Vezeridis MP. Liver metastases with 10 human colon carcinoma cell lines in nude mice and association with carcinoembryonic antigen production. *Cancer.* 1993;71:315–321.
13. Vogel CA, Galmiche MC, Westermann P, et al. Carcinoembryonic antigen expression, antibody localisation and immunophotodetection of human colon cancer liver metastases in nude mice: a model for radioimmunotherapy. *Int J Cancer.* 1996;67:294–302.
14. Warren RS, Yuan H, Matli MR, Gillett NA, Ferrara N. Regulation by vascular endothelial growth factor of human colon cancer tumorigenesis in mouse model of experimental liver metastasis. *J Clin Invest.* 1995;95:1789–1797.
15. Matsuoka Y, Kuroki M, Koga Y, Kuriyama H, Mori T, Kosaki G. Immunochemical differences among carcinoembryonic antigen in tumor tissues and related antigens in meconium and adult feces. *Cancer Res.* 1982;42:2012–2018.
16. Kuroki M, Arakawa F, Higuchi H, et al. Epitope mapping of the carcinoembryonic antigen by monoclonal antibodies and establishment of a new improved radioimmunoassay system. *Jpn J Cancer Res (GANN).* 1987;78:386–396.
17. Hunter WN, Greenwood FC. Preparation of iodine-131-labeled human growth hormone of high specific activity. *Nature.* 1962;194:495–496.
18. Brechbiel MW, Gansow OA, Atcher RW, et al. Synthesis of 1-(p-isothiocyanatobenzyl) derivatives of DTPA and EDTA. Antibody labeling and tumor-imaging studies. *Inorg Chem.* 1986;25:2772–2781.
19. Esteban JM, Schlom J, Gansow OA, et al. New method for the chelation of indium-111 to monoclonal antibodies: biodistribution and imaging of athymic mice bearing human colon carcinoma xenografts. *J Nucl Med.* 1987;28:861–870.
20. Yao Z, Sakahara H, Zhang M, et al. Radioimmunoimaging of colon cancer xenografts with anti-Tn monoclonal antibody. *Nucl Med Biol.* 1995;22:199–203.
21. Lindmo T, Boven E, Cuttitta F, Fedorco J, Bunn PA Jr. Determination of the immunoreactive fraction of radiorabeled monoclonal antibodies by linear extrapolation to binding at infinite antigen excess. *J Immunol Methods.* 1984;72:77–89.
22. Saga T, Weinstein JN, Jeong JM, et al. Two-step targeting of experimental lung metastases with biotinylated antibody and radiolabeled streptavidin. *Cancer Res.* 1994;54:2160–2165.

23. Jain RK, Baxter LT. Mechanisms of heterogeneous distribution of monoclonal antibodies and other macromolicules in tumors: significance of elevated interstitial pressure. *Cancer Res.* 1988;48:7022–7032.
24. Hagan PL, Halpern SE, Dillman RO, et al. Tumor size: effect on monoclonal antibody uptake in tumor models. *J Nucl Med.* 1986;27:422–427.
25. Boucher Y, Leuning M, Jain RK. Tumor angiogenesis and interstitial hypertension. *Cancer Res.* 1996;56:4264–4266.
26. Weinstein JN, Eger RR, Covell DG, et al. The pharmacology of monoclonal antibodies. *Ann NY Acad Sci.* 1987:507;199–210.
27. Fujimori K, Covell DG, Fletcher JE, Weinstein JN. A modeling analysis of monoclonal antibody percolation through tumors: a binding-site barrier. *J Nucl Med.* 1990;31:1191–1198.
28. Saga T, Neumann RD, Heya T, et al. Targeting cancer micrometastases with monoclonal antibodies: a binding-site barrier. *Proc Natl Acad Sci USA.* 1995;92: 8999–9003.
29. Chatal JF, Saccavini JC, Gestin JF, et al. Biodistribution of indium-111-labeled OC 125 monoclonal antibody intraperitoneally injected into patients operated on for ovarian carcinomas. *Cancer Res.* 1989;49:3087–3094.
30. Vogel CA, Galmiche MC, Buchegger F. Radioimmunotherapy and fractionated radiotherapy of human colon cancer liver metastases in nude mice. *Cancer Res.* 1997;57:447–453.
31. Mach J-P, Pèlegrin A, Buchegger F. Imaging and therapy with monoclonal antibodies in non-hematopoietic tumors. *Curr Opin Immunol.* 1991;3:685–693.
32. Buchegger F, Haskell CM, Schreyer M, et al. Radiolabeled fragments of monoclonal antibodies against carcinoembryonic antigen for localization of human colon carcinoma grafted into nude mice. *J Exp Med.* 1983;158:413–427.
33. Vogel CA, Bischof-Delaloye A, Mach JP, et al. Direct comparison of a radioiodinated intact chimeric anti-CEA MAb with its $F(ab')^2$ fragment in nude mice bearing different human colon cancer xenografts. *Br J Cancer.* 1993;68:684–690.
34. Buchegger F, Pfister C, Fournier K, et al. Ablation of human colon carcinoma in nude mice by ^{131}I-labeled monoclonal anti-carcinoembryonic antigen antibody $F(ab')^2$ fragments. *J Clin Invest.* 1989;83:1449–1456.
35. Zhu H, Baxter LT, Jain RK. Potential and limitation of radioimmunodetection and radioimmunotherapy with monoclonal antibodies. *J Nucl Med.* 1997;38:731–741.
36. Order SE, Sleeper AM, Stillwagon GB, Klein JL, Leichner PK. Radiolabeled antibodies: results and potential in cancer therapy. *Cancer Res.* 1990;50(Suppl.): 1011s–1013s.
37. LeBerthon B, Khawli LA, Alauddin M, et al. Enhanced tumor uptake of macromolecules induced by a novel vasoactive interleukin 2 immunoconjugate. *Cancer Res.* 1991;51:2694–2698.
38. Kuhn JA, Beatty BG, Wong JYC, et al. Interferon enhancement of radioimmunotherapy for colon carcinoma. *Cancer Res.* 1991;51:2335–2339.
39. Neta R, Douches S, Oppenheim JJ. Interleukin 1 is a radioprotector. *J Immunol.* 1986;136:2483–2485.
40. Lloyd JO. Tumor necrosis factor: another chapter in the long history of endotoxin. *Nature.* 1987;330:602–603.
41. Sharkey RM, Blumenthal RD, Behr TM, et al. Selection of radioimmunoconjugates for the therapy of well-established or micrometastatic colon carcinoma. *Int J Cancer.* 1997;72:477–485.
42. Denardo SJ, Richman CM, Goldstein DS, et al. Yttrium-90/indium-111-DOTA-peptide-chimeric L6: pharmacokinetics, dosimetry and initial results in patients with incurable breast cancer. *Anticancer Res.* 1997;17:1735–1744.